Journal of Nanoparticle Research **3:** 309–319, 2001.

Nanoparticle microreactor: Application to synthesis of titania by thermal decomposition of titanium tetraisopropoxide

K.Y. Park**, M. Ullmann, Y.J. Suh and S.K. Friedlander*
Department of Chemical Engineering, University of California, Los Angeles, CA 90095, USA
**Author for correspondence (Tel.: 310 825 2206; Fax: 310 206 4107; E-mail: skf@seas.ucla.edu)*

Received 5 January 2001; accepted in revised form 25 May 2001

Key words: nanoparticle microreactor, gas phase synthesis, nucleation, TiO_2, titanium tetraisopropoxide

Abstract

The nanoparticle microreactor (NPMR) is a new concept that we have introduced to describe a very small-scale system capable of converting an aerosol precursor to solid particles. The liquid precursor of about 1 μl is injected by a syringe through a septum into a tubular evaporator of 1.0 cm^3 in volume with stopcocks at both ends. The evaporator has been preheated by a heating tape to a temperature sufficiently high for vaporization to occur in half a minute. By opening the stopcocks, the vaporized precursor is transported by a carrier gas stream into a quartz tube which is mounted along the axis of a tubular furnace. The nanoparticle aggregates produced in the reactor are sampled by deposition on an electron micrograph grid at the reactor exit. The NPMR was applied first to the synthesis of TiO_2 particles by thermal decomposition of titanium tetraisopropoxide (TTIP) in a nitrogen carrier gas, with TTIP concentrations varying from 1.0 to 7.0 mol% or 2.35×10^{-6} to 1.65×10^{-5} in TiO_2 volume loading, and decomposition temperatures from 300°C to 1000°C. Studies were made with a 2 mm reaction tube and a 4 mm tube with sheath gas. With the 2 mm tube, a considerable fraction of the TTIP precursor was consumed at the wall by surface reaction, resulting in very small particles. With the 4 mm tube, the primary particle size was comparable to that reported in the literature for steady flow experiments using a 22.2 mm tube. Primary particle sizes ranged from 200 to 400 nm. Depending on TTIP concentration and reactor temperature, the particles exhibited a bimodal size distribution, probably due to a two-stage nucleation. A fourfold increase in the gas flow rate had little effect on particle size, indicating that particle growth ended early, within one-fourth the tube length. Residence time in the reactor was between 0.35 and 1.4 s, and total run time about 1 min. The NPMR has potential for rapid assembly of large databases and is adaptable to combinatorial discovery of nanoparticles with novel properties. Design requirements for an 'ideal' aerosol microreactor are discussed briefly.

Introduction

Gas phase synthesis of nanoparticles, in which a precursor is vaporized and reacts to form solid particles, is of interest because of its simplicity and ability to generate dry particles directly, compared to liquid phase synthesis. Carbon black, fumed silica and titania are important examples of nanoparticles produced commercially using gas phase synthesis. At the present time, considerable effort is being made to extend its application to the production of advanced powdered materials for use as catalysts, electronic devices and ductile ceramics. Many lab-scale studies have been made to demonstrate novel methods of particle synthesis or elucidate the mechanisms of particle formation, using a variety of reactors: flame, electrically heated, laser or plasma reactors (Pratsinis & Kodas, 1993). These studies have been made with a continuous supply of precursor vapor to the reactor; in most cases, a carrier gas was bubbled through the liquid precursor.

**On leave from Kongju National University, Kongju, Korea

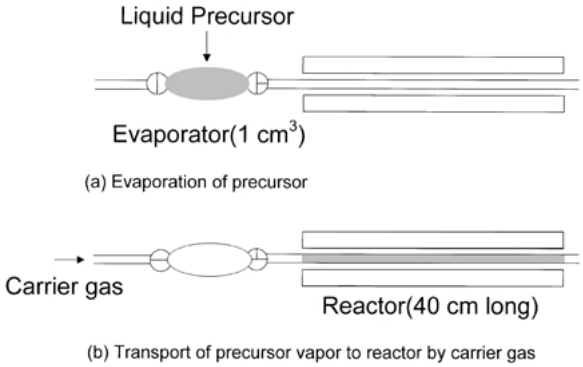

Figure 1. Concept of nanoparticle microreactor (precursor vapor is indicated in gray).

This method provides reliable data in steady state operation. However, it is less satisfactory for very small volumes of precursor and may be too time-consuming for rapid searching of product properties for new materials and varying process conditions. The search can be made more efficient by using small-scale reactors with short run time. An idea is to have a small volume of precursor vapor converted to particles, ideally under conditions of uniform temperature, concentration and residence time.

In the present work, a nanoparticle microreactor (NPMR) was developed which can accept a microliter of precursor and complete a run within a minute. Figure 1 shows the concept of the microreactor. The liquid precursor is injected into an evaporator, 1 cm^3 in volume and vaporized. Then, the precursor vapor is transported by a carrier gas to the reactor as a bolus, similar to a pulse injection. The reaction volume of the vapor is as small as 1 cm^3 and the reaction time is only a few seconds. Because of the small system size, NPMR operating conditions can easily and quickly be varied to produce large databases relating product properties (for example, particle size and crystal structure), to precursor properties and process conditions. These databases should be useful for discovery of nanoparticles with novel properties. This is an application of the combinatorial approach, which the pharmaceutical industry uses for the rapid synthesis and screening of new drug candidates (Dagani, 1999). Another advantage of the NPMR is that chemical consumption is smaller, producing fewer pollutants.

The NPMR was tested on the synthesis of TiO_2 particles from titanium tetraisopropoxide (TTIP) over the reaction temperature from 300°C to 1000°C, using two reaction tubes: a simple 2 mm tube and a 4 mm tube with sheath gas entry. Earlier studies of TiO_2 from TTIP using tubular reactors have been made by Kirkbir and Komiyama (1987), Okuyama et al. (1986) and Jang and Friedlander (1998). In these studies, however, the reaction tubes were an order of magnitude larger, 13–22.2 mm in diameter, and the precursor was transported to the reactor continuously by a carrier gas bubbled through a bottle containing liquid TTIP. Another difference is in the concentration of TTIP; in the present study concentration ranged from 1.0 to 7.0 mol%, much higher than those of previous studies ranging from 0.00136 to 1.34 mol%. A concentration of 7.0 mol% is in the range typical of silica flame synthesis in industrial reactors (Ulrich, 1971); data in commercial reactors for TiO_2 were not available to us. The production of TiO_2 by thermal decomposition of TTIP was experimentally validated earlier at a temperature higher than 250°C (Komiyama et al., 1984). We assume that the solid decomposition product of the present study made at 300–1000°C is TiO_2. In the present paper, the particle size was chosen for discussion, out of various product properties. The effects of tube size, TTIP concentration, reactor temperature and residence time on the primary particle size were investigated. The particle sizes were compared with those of Kirkbir and Komiyama (1987), who bubbled helium through the liquid precursor and passed the mixed vapors through a 22.2 mm reaction tube. Our goal was to study the effect of scale and batch vs. continuous operation on product properties.

Experimental section

Nanoparticle microreactor system

Figure 2 shows a schematic diagram of the microreactor system which consists of an oxygen trap (Hewlett-Packard, Model HP3150-0528), a drying column (Hammond, Model 27066) a carrier gas preheater, an evaporator, a tubular furnace (Thermolyne, Model 21100) and a particle collector. The preheater is a pyrex cylinder wrapped with a heating coil, with a volume of 100 cm^3 selected to give a residence time of 3 min at the carrier gas rate of 34 cm^3/min. The carrier gas is heated by the preheater to a temperature higher by about 20°C than the evaporation temperature to protect the vapor generated in the evaporator from being condensed by the incoming carrier gas. The evaporator is a pyrex tube with stopcocks at both ends, measuring 0.5 cm I.D. and 5 cm long. A septum is placed in the center for injection of liquid precursor by a syringe. The evaporator was

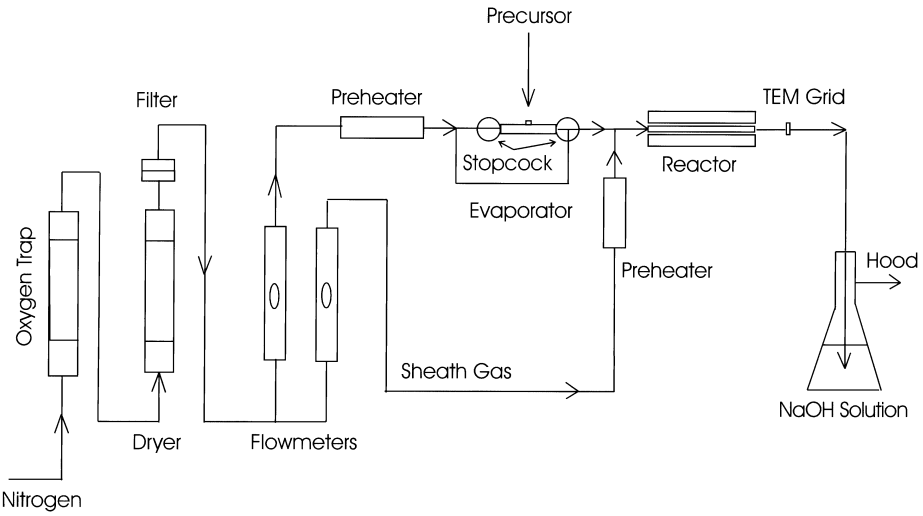

Figure 2. Schematic drawing of nanoparticle microreactor system.

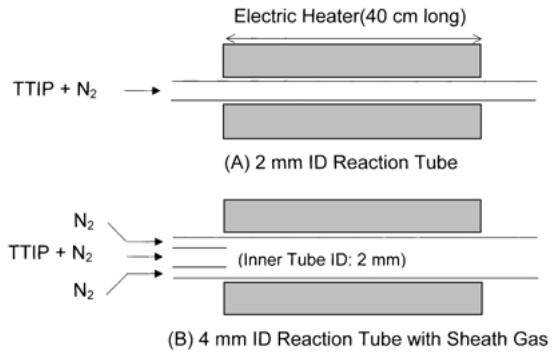

Figure 3. Two types of reaction tube used in the present study.

wrapped with a heating coil, and the temperature monitored by a thermocouple inserted through the septum. The evaporator was heated to a predetermined temperature before evaporation began. To start the evaporation, the two stopcocks were closed and the precursor injected by a syringe. By opening the stopcocks simultaneously, a bolus of the precursor vapor is transported to the reactor by the carrier gas. During evaporation, the carrier gas bypasses the evaporator through the three-way stopcock on the right hand side.

The reactor is a quartz tube 45 cm long, mounted along the axis of an electric furnace. Figure 3 shows the two reaction tubes used in our study. In the case of the 2 mm tube, one end is connected to the evaporator and the other end to the particle collector by O-ring ball joints. The distance from the evaporator outlet to the furnace inlet is about 10 cm. For the 4 mm tube with sheath gas, a 1/4-inch stainless steel union cross was added for the introduction of sheath gas, between the evaporator and the furnace (Figure 4). The sheath gas preheated in a heating pipe comes from the bottom of the union cross, turns to the right and passes through a 80 mesh screen, and enters the 4 mm tube to form a sheath layer outside the TTIP stream leaving the 2 mm inner tube. The union cross is wrapped with a heating tape and a thermocouple is installed to measure the sheath gas temperature.

At the reactor exit, a transmission electron microscopy (TEM) grid about 3 mm in diameter was mounted on a stainless steel tube and inserted into the center of the aerosol stream. Particle deposition took place probably by diffusion to the surface of the grid from the gas flowing along the axis of the reactor tube. After completion of a run (about 1 min) the grid holding tube was removed through an O-ring.

Experimental procedure

Nitrogen (99.99%) was passed through the oxygen trap and dryer in series and split into two streams: one to the carrier gas preheater and the other to the sheath gas preheater. The flow rate of each stream was measured by a rotameter before the preheater. The sheath gas flow rate was three times the carrier gas flow rate to keep the linear velocity of each stream the same at the entrance to the reaction tube. The carrier gas was preheated to 170°C in the preheater and passed through the evaporator with the stopcocks open for about

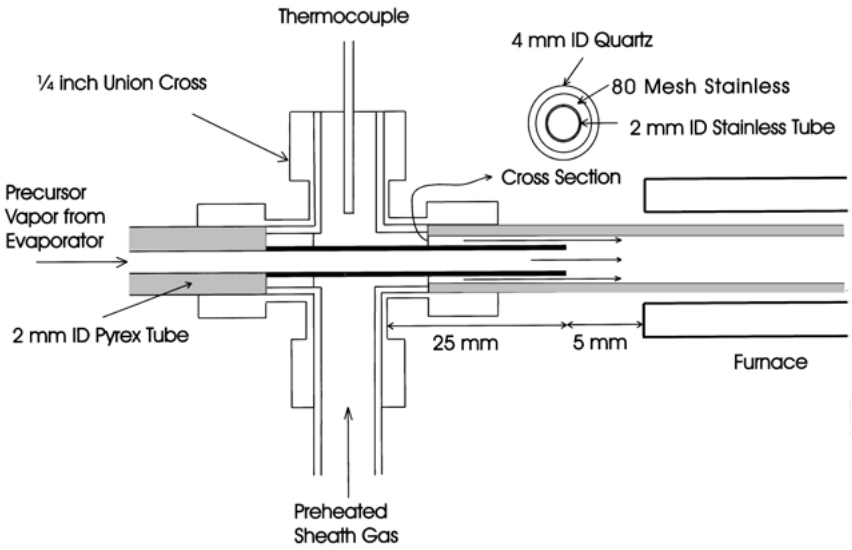

Figure 4. Illustration of sheath gas entry section. Inside the union cross, a 2 mm stainless steel tube, 64 mm in length and 0.2 mm in thickness, is installed extending into the 4 mm reaction tube by 25 mm.

30 min until the evaporator was purged and heated to 152°C, 10°C higher than the saturation temperature at the maximum TTIP concentration of 7 mol%. Then, the stopcocks were closed and a predetermined volume of TTIP was injected into the evaporator by a 1 μl syringe (SGE, Model SG-000500). The TTIP was of ultra high purity (99.999%, Sigma-Aldrich). The volume of TTIP required for a concentration of 7 mol% in the reactor gas flow was 0.7 μl. The concentration was controlled by the injection volume of TTIP.

The time to vaporize the TTIP was estimated to be 53 s, assuming that the 1 mm TTIP droplet remaining suspended from the tip of the syringe during the entire period of evaporation. In reality, the drop may fall to the evaporator wall during heating, due to the decrease of surface tension. Based on the estimate, the residence time in the evaporator was varied from 5 to 30 and 60 s, with the reactor temperature at 700°C. Particle size was smaller with a residence time of 5 s indicating the time is too short for complete vaporization. There was no difference in particle size for residence times between 30 and 60 s; therefore, the evaporation time was kept at 30 s.

The stopcocks were opened immediately after evaporation to transport the TTIP vapor to the reactor which had already been heated to a predetermined temperature. The power to the heating tape wrapping the transport line was controlled to maintain the vapor temperature at about 170°C, well above the saturation temperature. The operating conditions for the experiments are shown in Table 1.

Table 1. Operating conditions

Operating parameter	For 2 mm tube	For 4 mm tube with sheath gas
TTIP conc. (mol%)	7.0	1.0–7.0
N_2 carrier flow rate (cm^3/min)	34.0	17.0–68.0
N_2 sheath flow rate (cm^3/min)	0.	51.0–204.0
Space time at STP (s)	2.2	1.1–4.4
Reactor temp. (°C)	500–1000	300–700
Evaporator volume: 1.0 cm^3		
Evaporator temperature: 152°C		
Evaporation time: 30 s		
Operating pressure: 101.3 kPa		

At the exit from the reactor, the particles were collected on the carbon film coating a 200 mesh nickel grid (Electron Microscopy Science, Model CF200-Ni), and examined by transmission electron microscopy (JEOL, Model JEM 100CX). The particles were present both as individual primary particles and aggregates. From an image obtained by scanning the TEM micrograph, 70–200 primary particles were selected and their sizes were determined to calculate the number average and Sauter mean diameters using a computer program in which the number of pixels occupied by a particle is counted and converted into a diameter. The Sauter mean

diameter, D_{32} is defined as $\sum N_i d_i^3 / \sum N_i d_i^2$, where N_i is the number of particles of diameter d_i. It was used earlier by Kirkbir and Komiyama (1987) and employed for comparison purposes.

Results and discussion

Two millimeter reaction tube

Figure 5 shows the change in primary particle size for the 2 mm reaction tube, as the reactor temperature was increased from 500°C to 700°C and 1000°C. A constant temperature zone about 30 cm long was maintained in the reaction tube. The Sauter mean diameter of the primary particles increased with reactor temperature from 9.0 nm at 500°C to 20.6 nm at 700°C and 31.7 nm at 1000°C. Compared to those of Kirkbir and Komiyama (1987), 120 nm at 500°C and 65 nm at 700°C, our primary particle size is much smaller even though our TTIP concentration was 10 times higher, and the effect of the temperature on particle size is in the opposite direction. We set out to determine the cause of the discrepancy.

The TTIP concentration, initially 7 mol% in the evaporator, decreases due to dispersion as the bolus moves from the evaporator to the reactor. By a rough calculation, the dispersion must have affected the particle size to some extent, but was probably not the critical factor causing the discrepancy. After the run, inspection of the wall of the 2 mm tube showed a zone coated with what was probably TiO_2. At a reactor temperature of 500°C, a coated zone 2.2 cm in length formed starting at 1.2 cm from the furnace inlet (Figure 6). The length of coated zone was decreased to 0.7 cm by an increase of the reactor temperature to 700°C. A considerable portion of the TTIP vapor admitted to the reaction tube probably reacted at the wall, reducing the amount of TTIP available for particle formation. This may be the main reason why our primary particle sizes with the 2 mm reaction tube were much smaller than those of the earlier studies. As the temperature increased, the rate of homogeneous reaction in the gas phase increased, and the TTIP loss to the wall decreased, leading to an increase in particle size.

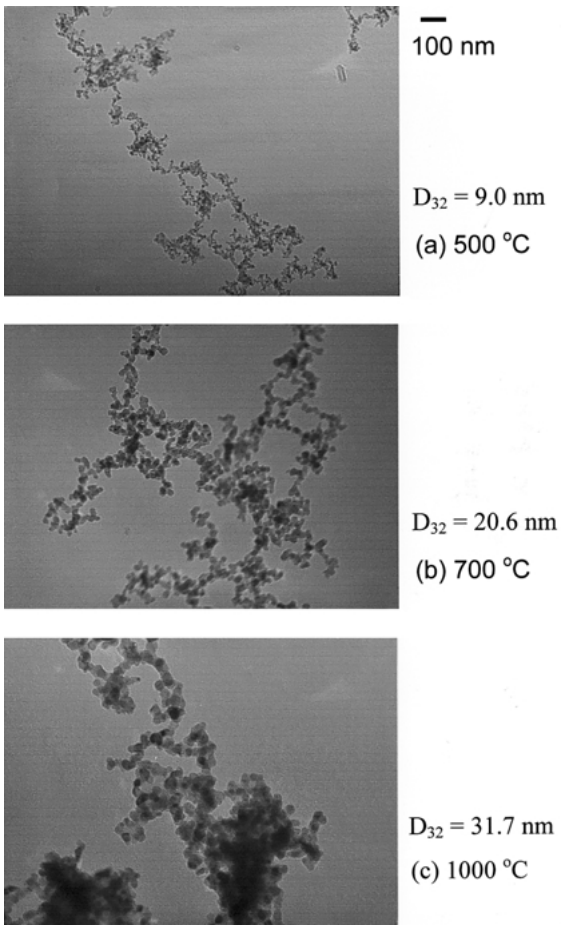

Figure 5. TEM images of TiO_2 particles with 2 mm reaction tube (N_2 flow: 34 cm^3/min; TTIP concentration: 7 mol%). D_{32} is the Sauter mean primary particle diameter. Most of the TTIP conversion took place on the reactor wall.

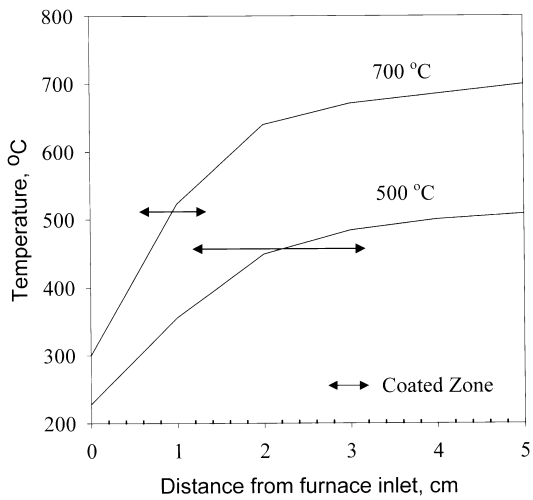

Figure 6. Temperature profile and location of coated zones with 2 mm reaction tube.

The coalescence of colliding particles may also have played a role in the particle size increase with the temperature increase to 1000°C; the collision-coalescence mechanism described earlier by our group (Windeler et al., 1997) predicts significant coalescence at this temperature. At a reaction temperature of 1000°C, another zone coated with black carbonaceous materials formed, probably by decomposition of propylene, a byproduct of TTIP decomposition. The leaf-like features seen in the TEM micrograph at 1000°C (Figure 5c) may be the carbonaceous materials.

Four millimeter reaction tube with sheath gas

To reduce the surface-reaction effect, the 2 mm reaction tube was replaced by a 4 mm tube with sheath gas entry. As shown in Figure 3, sheath nitrogen was introduced to protect the wall from being coated by surface reaction. The carrier gas flow rate was kept the same as with the 2 mm tube. The sheath gas rate was controlled such that its average linear velocity was the same as that of the TTIP stream leaving the inner 2 mm tube. After a run, no coated zone was seen. After a few more runs, a coated zone became visible indicating that the surface reaction at the wall was not eliminated completely. Kirkbir and Komiyama (1987) reported earlier that a coated zone formed even with a much larger tube, 22 mm in diameter, in the absence of sheath gas. The precursor loss to some extent by surface reaction seems to be unavoidable in laboratory-scale reactors. In the present study, it was difficult to measure the loss because of the small volume of precursor admitted to the reactor.

Figure 7 shows the TEM micrographs of particles produced with reactor temperatures varying from

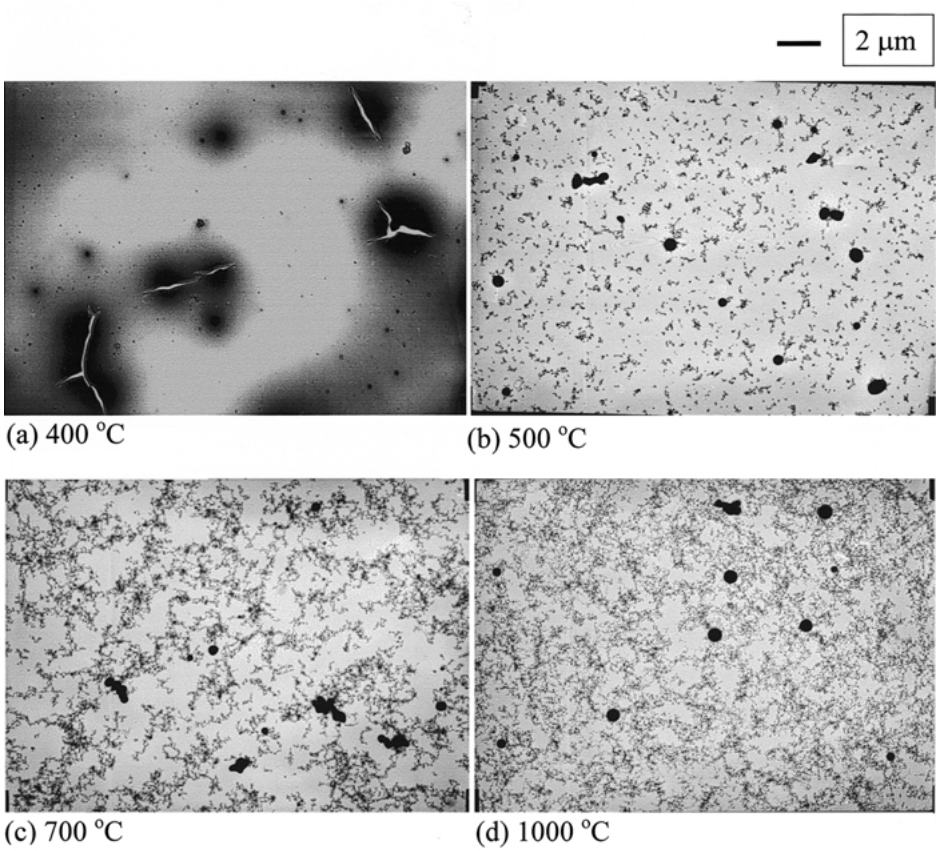

Figure 7. Effect of reactor temperature on particle morphology for 4 mm reaction tube with sheath gas (N_2 carrier gas: 34 cm^3/min; TTIP concentration: 7 mol%).

400°C to 1000°C, holding the TTIP concentration at 7 mol% and the carrier gas rate at 34 cm^3/min. At temperatures higher than 500°C, the particle size showed a bimodal distribution: one group of larger spherical particles, 250–650 nm in diameter and the other group of chain-like aggregates composed of 15–20 nm particles. At 400°C, however, those chain aggregates disappeared, indicating that the aggregates were generated between 400°C and 500°C. The cracks seen around the particles at 400°C (Figure 7a) formed in a few seconds after the TEM grid was placed under an illumination of electron beam for examination. Some unconsolidated materials may have deposited around the particles and undergone a structural change under the beam to develop a stress resulting in the formation of the cracks. Figure 8 shows the effect of TTIP concentration on particle morphology. The concentration was varied from 7 to 3.5 and 1.0 mol%, keeping the reactor temperature constant at 700°C and the carrier gas flow rate at 34 cm^3/min. As the concentration was reduced from 7 to 3.5 mol%, the length and the number of the aggregates decreased markedly. The chain aggregates finally disappeared as the concentration was further reduced to 1 mol%.

The bimodal size distribution has not been reported in previous studies, which were performed at TTIP concentrations much lower than in the present study and with larger reaction tubes. To elucidate the cause of the bimodal distribution, it may be necessary to understand the mechanism by which the decomposition occurs. The overall reaction can be represented by $Ti(OC_3H_7)_4 = TiO_2 + 4C_3H_6 + 2H_2O$. However, the reaction mechanism is not well known yet. By analogy to the mechanism of tetraethoxysilane (TEOS) decomposition (Satake et al., 1996), we assume that the decomposition of TTIP proceeds as follows by (1) β-hydride elimination of propene and

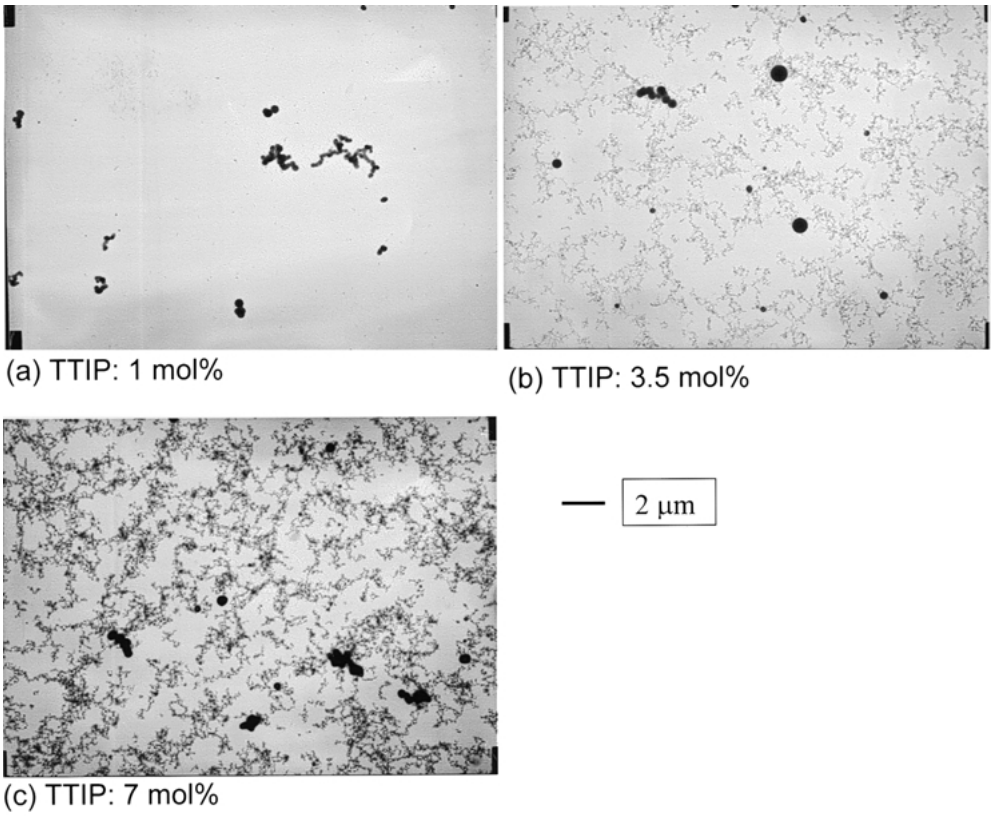

Figure 8. Effect of TTIP concentration on particle morphology for 4 mm reaction tube with sheath gas (N_2 carrier gas: 34 cm^3/min; Reactor temperature: 700°C).

(2) polymerization:

$$(CH_3CHCH_3O)_3Ti(OCH_3CHCH_3) \rightarrow (CH_3CHCH_3O)_3Ti(OH) + CH_2CHCH_3 \quad (1)$$

$$(CH_3CHCH_3O)_3Ti(OH) + (CH_3CHCH_3O)Ti(OCH_3CHCH_3)_3 \rightarrow (CH_3CHCH_3O)_3Ti\text{–}O\text{–}Ti(OCH_3CHCH_3)_3 + CH_3CH(OH)CH_3 \quad (2)$$

By successive β-hydride elimination and polymerization, the dimeric species in Eq. (2) continues to grow with its vapor pressure decreasing, and eventually leads to a stable particle or a nucleus when the vapor pressure drops below a certain level. The nucleus may not be pure TiO_2, but contain carbon and hydrogen to some extent. Once nuclei are formed, they grow by surface reaction of TTIP vapor and scavenging of the clusters and by coagulation as well. During the growth, residual carbon and hydrogen are removed by further decomposition to make TiO_2. The isopropyl alcohol in Eq. (2) is dehydrated to produce propene and water. TiO_2 is known to catalyze the dehydration (Carrizosa & Munuera, 1977).

TTIP vapor decomposes at temperatures above 250°C (Fictorie et al., 1994). Komiyama et al. (1984) reported a similar decomposition temperature. Figure 9 shows the temperature profile measured at a reactor set point of 500°C, over the transient zone where the temperature is on the increase. The approximate concentration profile shown in the figure illustrates the discussion that follows. The TTIP vapor admitted at 200°C to the 4 mm tube starts to be heated and decomposition begins. Nucleation occurs when the gas is heated to a sufficiently high temperature. This temperature is not known, but may be between 250°C and 400°C. The nuclei, then, grow as described above. When the vapor temperature reaches 400°C, further nucleation occurs provided that a sufficient amount of TTIP vapor remains unconsumed. The larger particles in Figures 7 and 8 may have originated from the first nucleation and the smaller particles composing the chain aggregates from the second nucleation.

The second nucleation rate may be faster than the first because of the higher temperature generating more nuclei resulting in smaller primary particles. At the TTIP concentration of 1 mol% and the reactor temperature of 700°C (Figure 8a), the second nucleation did not occur because the amount of TTIP left after the first nucleation and subsequent growth was not enough to generate new particles. At the reactor temperature of 400°C and the TTIP concentration of 7 mol% (Figure 7a), the second nucleation did not take place either because the temperature was too low, even though the TTIP concentration was high enough. In the synthesis of silicon from silane (SiH_4), Alam and Flagan (1986) reported that undesired nucleation could be avoided by controlling the temperature profile in the reactor. Experimental evidence that the heating rate in the early stages affected particle size can also be found in the work of Park et al. (1991) on the generation of iron particles by hydrogen reduction of $FeCl_2$ vapor. Thus, the temperature profile in the transient zone must be a factor in controlling the particle size.

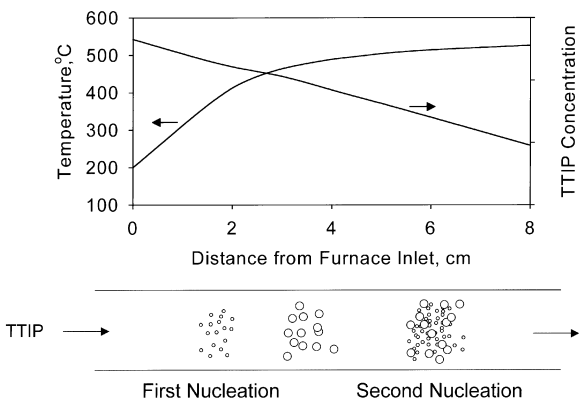

Figure 9. Two-stage nucleation in furnace.

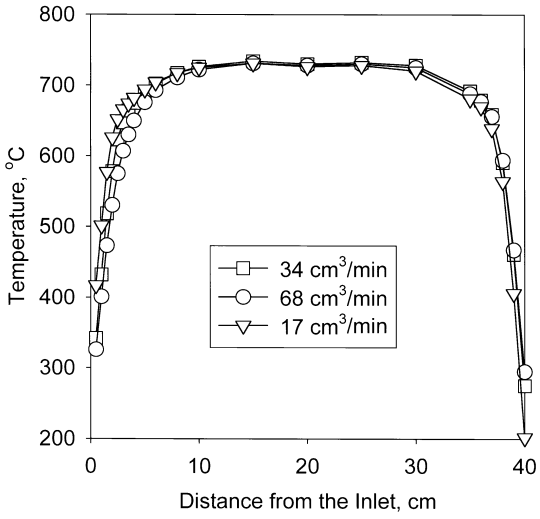

Figure 10. Axial temperature profiles with varying carrier gas flow rates at 700°C for 4 mm reaction tube with sheath gas.

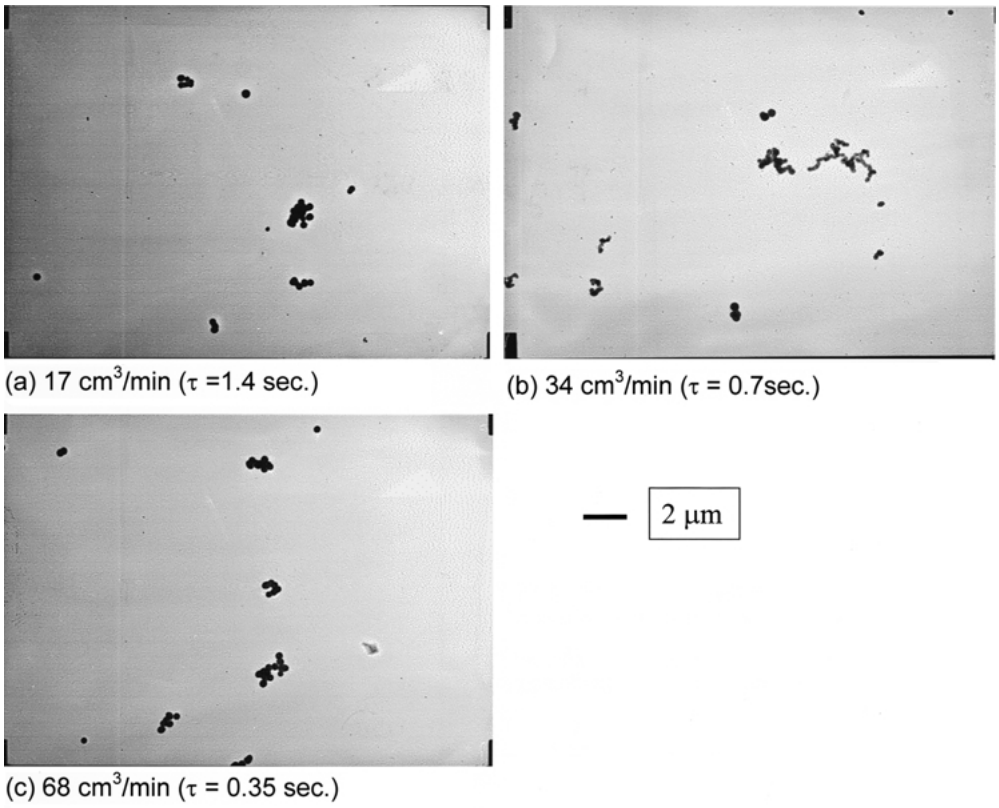

Figure 11. Effect of carrier gas flow rate on particle size for 4 mm reaction tube with sheath gas (reactor temperature: 700°C; TTIP concentration: 1 mol%). The residence time, τ (reactor volume/volumetric flow rate at 700°C), varied from 0.35 to 1.4 s. There was no effect of residence time on primary particle size.

Holding the reactor temperature at 700°C and the TTIP concentration at 1 mol%, the carrier gas flow rate was varied from 17 to 68 cm^3/min, while maintaining the ratio of sheath to carrier gas rates at 3.0. The temperature profiles with varying gas flow rates are shown in Figure 10. There exist some temperature differences in the transient zone, between the three gas flow rates, but nearly no difference in the isothermal zone. Figure 11 shows that the particle size is insensitive to the variation of the gas rate or the increase of the residence time by a factor of four. This implies that the particle growth was completed within one-fourth of the tube length. A similar result was reported by Kirkbir and Komiyama (1987) who found that the variation of the residence time in the range 3.8–10.2 s had no effect on the particle diameter of TiO_2 produced from TTIP at 300°C. In contrast, Akhtar et al. (1991) reported that for TiO_2 particles generated by oxidation of $TiCl_4$ in a tubular reactor, particle size increased with increasing residence time at a reactor temperature of 1123°C. They attributed the size increase to an increase in time for coagulation. The reactor temperature of the present study may be too low for coalescence to occur; once the primary particles formed, the residence time had little effect on their size.

Comparison with results from a steady flow larger scale system

A principal goal of our study was to compare the microreactor data with results for larger scale systems. For this purpose, the primary particle sizes were compared with results of Kirkbir and Komiyama (1987) whose tube size was larger, 22.2 mm in diameter, with the precursor vapor supplied steadily to the reactor by bubbling helium through a precursor reservoir. Figure 12 shows the comparison for TTIP concentrations near 1.0 mol% with reactor temperatures ranging from 300°C to 700°C. The concentration indicated

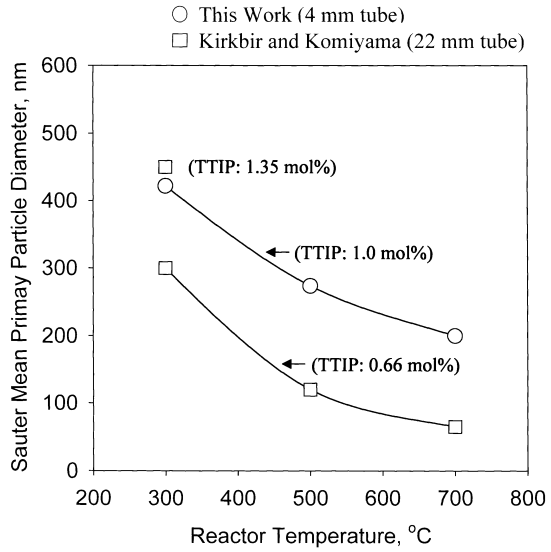

Figure 12. Comparison of primary particle size for the NPMR and a larger scale system.

for our data is the one at the evaporator. The actual concentration of TTIP in the reaction zone must be lower because the TTIP vapor disperses during transport from the evaporator to the reactor and diffuses to the sheath gas layer, on entering the reactor. At present, no quantitative information is available on the concentration decay.

Figure 12 shows that our particle sizes were comparable to the flow reactor data and the dependence of particle size on the temperature was similar, the particle size decreasing with increasing temperature. In the gas-phase synthesis of TiO_2 from TTIP or $TiCl_4$, some investigators (Suyama & Kato, 1976; Jang & Jeong, 1995) reported a similar decrease in particle diameter with increasing temperature, while other studies (Formenti et al., 1972; Akhtar et al., 1991) showed an increase. By examining the operating temperatures at which those data were obtained, the transition temperature was near 1100°C. At temperatures below 1100°C, the particle size seems to be controlled by the nucleation rate because the temperature is probably too low for significant coalescence of aggregates. Above 1100°C, coalescence becomes dominant, and the particle size increases with increasing temperature. Summarizing, an important factor in the scaling of these systems is the time–temperature history as well as the concentration of the precursor vapor; if these features are similar for different aerosol reactors, the particle size of the product should be similar.

Summary and conclusions

In aerosol reactor design, the main goal is to produce particles with desired properties – primary particle size, aggregate size, crystalline state and primary particle bond energies. It is generally not possible to predict particle properties from first principles alone, and pilot scale studies and modeling are important in scale-up. We have introduced the concept of a small-scale 'microreactor' capable of generating particle samples on TEM grids which are easily examined for particle properties.

To test this concept, we designed a miniaturized reactor capable of producing TiO_2 nanoparticles from about 1 μl of TTIP in a 1 min run time. With a 2 mm reaction tube, a considerable fraction of the TTIP was consumed at the wall by surface reaction, resulting in very small particles. For a 4 mm tube with sheath gas, the surface reaction was reduced and the particle size was comparable to that reported earlier by other investigators for steady flow experiments with a 22.2 mm tube. Increasing the gas flow rate by four times had little effect on particle size, implying that particle growth had been completed within one-fourth of the tube length, also in agreement with previous work using a larger reactor. Depending on TTIP concentration and reactor temperature, particles showed a bimodal size distribution probably due to a two-stage nucleation.

The microreactor has potential for the rapid assembly of large databases and is adaptable to combinatorial discovery of nanoparticles with novel properties. Results compare well over some ranges with a larger scale reactor. Still much work remains to be done to make the microreactor a reliable tool for predicting particle properties of larger scale systems. Accounting for axial dispersion requires further study. Rapid analysis of TEM grid particle deposits is another challenge.

Acknowledgements

This research was supported by the Korea Research Foundation Program for Support for Faculty Research Abroad and by NSF Grant #CTS9911133. S.K. Friedlander is Parsons Professor of Chemical Engineering.

References

Akhtar K.M., Y. Xiong & S.E. Pratsinis, 1991. Vapor synthesis of titania powder by titanium tetrachloride oxidation. AIChE J. 37, 1561–1570.

Alam M.K. & R.C. Flagan, 1986. Controlled nucleation aerosol reactors: Production of bulk silicon. Aerosol Sci. Technol. 5, 237–248.

Carrizosa I. & G. Munuera, 1977. Study of the interaction of aliphatic alcohols with TiO_2. I. Decomposition of ethanol, 2-propanol, and tert-butanol on anatase. J. Catal. 49, 174–188.

Dagani R., 1999. A faster route to new materials. Chem. Eng. News, 8 March, 1999, 51–60.

Fictorie C.P., J.F. Evans & W.L. Gladfelter, 1994. Kinetic and mechanistic study of the chemical vapor deposition of titanium dioxide thin films using tetrakis-(isopropoxo)-titanium(IV). J. Vac. Sci. Technol. A 12, 1108–1113.

Formenti M., F. Juillet, P. Meriaudeau, S.J. Teichner & P. Vergnon, 1972. Preparation in a hydrogen–oxygen flame of ultrafine metal oxide particles. In: Hidy G.M. ed. Aerosols and Atmospheric Chemistry. Academic Press, New York, pp. 45–54.

Jang H.D. & J. Jeong, 1995. The effects of temperature on particle size in the gas-phase production of TiO_2. Aerosol Sci. Technol. 23, 553–560.

Jang H.D. & S.K. Friedlander, 1998. Restructuring of chain aggregates of titania nanoparticles in the gas phase. Aerosol Sci. Technol. 29, 81–91.

Kirkbir F. & H. Komiyama, 1987. Formation and growth mechanism of porous, amorphous, and fine particles prepared by chemical vapor deposition. Titania from titanium tetraisopropoxide. Can. J. Chem. Eng. 65, 759–766.

Komiyama H., T. Kanai & H. Inoue, 1984. Preparation of porous, amorphous, and ultrafine TiO_2 particles by chemical vapor deposition. Chem. Lett. 1984, 1283–1286.

Okuyama K., Y. Kousaka, N. Tohge, S. Yamamoto, J.J. Wu, R.C. Flagan & J.H. Seinfeld, 1986. Production of ultrafine metal oxide aerosol particles by thermal decomposition of metal alkoxide vapors. AIChE J. 32, 2010–2019.

Park K.Y., H.D. Jang & C.S. Choi, 1991. Generation of ultrafine iron powders by gas-phase reduction of ferrous chloride with hydrogen. J. Aerosol Sci. 22, S113–S116.

Pratsinis S.E. & T.T. Kodas, 1993. Manufacturing of materials by aerosol processes. In: Willeke K. & Baron P.A. eds. Aerosol Measurement. John Wiley, USA, pp. 721–746.

Satake T., T. Sorita & H. Adachi, 1996. Kinetic and theoretical study of the thermal decomposition of tetraethoxysilane in the gas phase. In: Besmann T.M., Allendorf M.D., Robinson Mc D. & Ulrich R.K. eds. Proceedings of the Thirteenth International Conference on Chemical Vapor Deposition, Los Angeles, CA, USA, 5–10 May, pp. 23–28.

Suyama Y. & A. Kato, 1976. TiO_2 produced by a vapor-phase oxygenolysis of $TiCl_4$. J. Am. Ceram. Soc. 59, 146–149.

Ulrich G.D., 1971. Theory of particle formation and growth in oxide synthesis flames. Combust. Sci. Technol. 4, 47–57.

Windeler R.S., Kari E.J. Lehtinen & S.K. Friedlander, 1997. Production of nanometer-sized metal oxide particles by gas phase reaction in a free Jet. II: Particle size with neck formation – comparison with theory. Aerosol Sci. Technol. 27, 191–205.